発表者氏名	論文タイトル名	発表誌名	巻号	ページ	出版年
Wakusawa K. et al., Haginoya K.	A girl with Cardio-facio-cutaneus syndrome complicated with status epileptics and acute encephalopathy.	Brain Dev	印刷中	未確定	2013
Kobayasi S. et al, Haginoya K.	A case of atypical benign partial epilepsy with action myoclonus.	Seizure	印刷中	未確定	2013
Abe Y. et al, Haginoya K.	Bilateral Periventricular Nodular Heterotopia with Megalencephaly: A Case Report.	J Child Neurol	印刷中	未確定	2013
Kakisaka Y. Haginoya K., et al	Additional Evidence That the Ryanodine Receptor Gene (RYR1) Causes Malignant Hyperthermia and Severe Skeletal Malformations.	Am J Med Genet	161	234-235	2013
Numata Y. et al., Haginoya K.	Brain magnetic resonance imaging, and motor and intellectual functioning in 86 patients born at term with spastic diplegia.	Dev Med Child Neurol.	55	167-172	2013
Yokoyama H, et al., Haginoya K. et al.	Ketotifen overdose in infancy associated with development of epilepsy and mild mental retardation.	Pediatr Int.	54(6)	963	2012
Zhao YJ, et al. Haginoya K.	Protective effects of glutamine in a rat model of endotoxemia.	Mol Med Report.	6	739-744	2012
Iwasaki M, et al. Haginoya K. et al.	Complete remission of seizures after corpus callosotomy.	J Neurosurg Pediatr.	10	7-13	2012
Watanabe S, et al. Haginoya K. et al.	Schinzel–Giedion syndrome: A further cause of early myoclonic encephalopathy and vacuolating myelinopathy.	Brain Dev	34	151-155	2012
Kakisaka Y, et al. Haginoya K.	Abdominal migraine revieved from both central and peripheral aspects.	World J Exp Med.	2	75-77	2012
Tsuburaya R, et al. Haginoya K. et al.	Unusual ribbon-like periventricular heterotopia with congenital cataract in a Japanese girl.	Am J Med Genet	158A	674-677	2012

発表者氏名	論文タイトル名	発表誌名	巻号	ページ	出版年
Uematsu M. Haginoya K. et al.	Hypoperfusion in caudate nuclei in patients with brain–lung–thyroid syndrome.	J Neurol Sci.	315	77-81	2012
Nakamura K. Kato M. et al.	Congenital dysplastic microcephaly and hypoplasia of the brainstem and cerebellum with diffuse intracranial calcification.	J Child Neurol	27	218-221	2012
Tanigawa J. et al. Osaka K	Two Japanese patients with Leigh syndrome caused by novel SURF1 mutations.	Brain Dev	印刷中	未確定	2013
Koizume S. et al., Osaka H. et al.	HIF2α-Sp1 interaction mediates a deacetylation-dependent FVII-gene activation under hypoxic conditions in ovarian cancer cells.	Nucleic Acids Res.	印刷中	未確定	2013
Yu LH. et al., Osaka H. Inoue K.	Effect of curcumin in a mouse model of Pelizaeus-Merzbacher disease.	Mol Genet Metab	106(1)	108-114	2012
Tomiyasu M. et al., Osaka H.	Monitoring the brain metabolites of children with acuteencephalopathy caused by the H1N1 virus responsible for the 2009 influenzapandemic: a quantitative in vivo (1)H MR spectroscopy study.	Magn Reson Imaging.	30(10)	1527-1533	2012
Kouga T., et al. Osaka H.	A Child with Three Episodes of Reversible Splenial Lesion.	Neuropediatrics.	印刷中	未確定	2013
Yoshihara N. et al. Osaka H.	Idiopathic cranial polyneuropathy with unilateral IX and X and contralateral XI nerve palsy in a 4-year-old boy.	Pediatr Neurol.	47(3)	198-200	2012
Kimura-Ohba S, et al. Osaka H. et al.	A case of cerebral hypomyelination with spondylo-epi-metaphyseal dysplasia.	Am J Med Genet	161(1)	203-207	2013

ORIGINAL ARTICLE

Phenotypic Spectrum of *COL4A1* Mutations: Porencephaly to Schizencephaly

Yuriko Yoneda, MSc,[1] Kazuhiro Haginoya, MD, PhD,[2,3] Mitsuhiro Kato, MD, PhD,[4] Hitoshi Osaka, MD, PhD,[5] Kenji Yokochi, MD, PhD,[6] Hiroshi Arai, MD,[7] Akiyoshi Kakita, MD, PhD,[8] Takamichi Yamamoto, MD, MS, DMSc,[9] Yoshiro Otsuki, MD, PhD,[10] Shin-ichi Shimizu, DDS, PhD,[10] Takahito Wada, MD, PhD,[5] Norihisa Koyama, MD, PhD,[11] Yoichi Mino, MD,[12] Noriko Kondo, MD,[13] Satoru Takahashi, MD, PhD,[14] Shinichi Hirabayashi, MD, PhD,[15] Jun-ichi Takanashi, MD, PhD,[16] Akihisa Okumura, MD, PhD,[17] Toshiyuki Kumagai, MD,[18] Satori Hirai, MD,[7] Makoto Nabetani, MD,[19] Shinji Saitoh, MD, PhD,[20] Ayako Hattori, MD, PhD,[20] Mami Yamasaki, MD, PhD,[21] Akira Kumakura, MD,[22] Yoshinobu Sugo, MD,[1] Kiyomi Nishiyama, PhD,[1] Satoko Miyatake, MD, PhD,[1] Yoshinori Tsurusaki, PhD,[1] Hiroshi Doi, MD, PhD,[1] Noriko Miyake, MD, PhD,[1] Naomichi Matsumoto, MD, PhD,[1] and Hirotomo Saitsu, MD, PhD[1]

Objective: Recently, *COL4A1* mutations have been reported in porencephaly and other cerebral vascular diseases, often associated with ocular, renal, and muscular features. In this study, we aimed to clarify the phenotypic spectrum and incidence of *COL4A1* mutations.

Methods: We screened for *COL4A1* mutations in 61 patients with porencephaly and 10 patients with schizencephaly, which may be similarly caused by disturbed vascular supply leading to cerebral degeneration, but can be distinguished depending on time of insult.

Results: *COL4A1* mutations were identified in 15 patients (21%, 10 mutations in porencephaly and 5 mutations in schizencephaly), who showed a variety of associated findings, including intracranial calcification, focal cortical dysplasia, pontocerebellar atrophy, ocular abnormalities, myopathy, elevated serum creatine kinase levels, and hemolytic anemia. Mutations include 10 missense, a nonsense, a frameshift, and 3 splice site mutations. Five mutations were confirmed as de novo events. One mutation was cosegregated with familial porencephaly, and 2

View this article online at wileyonlinelibrary.com. DOI: 10.1002/ana.23736

Received Jun 8, 2012, and in revised form Aug 6, 2012. Accepted for publication Aug 10, 2012.

Address correspondence to Dr Saitsu, Department of Human Genetics, Yokohama City University Graduate School of Medicine, 3-9 Fukuura, Kanazawa-ku, Yokohama 236-0004, Japan. E-mail: hsaitsu@yokohama-cu.ac.jp

From the [1]Department of Human Genetics, Yokohama City University Graduate School of Medicine, Yokohama; [2]Department of Pediatrics, Tohoku University School of Medicine, Sendai; [3]Department of Pediatric Neurology, Takuto Rehabilitation Center for Children, Sendai; [4]Department of Pediatrics, Yamagata University Faculty of Medicine, Yamagata; [5]Division of Neurology, Clinical Research Institute, Kanagawa Children's Medical Center, Yokohama; [6]Department of Pediatric Neurology, Seirei-Mikatahara General Hospital, Hamamatsu; [7]Department of Pediatric Neurology, Morinomiya Hospital, Osaka; [8]Department of Pathology, Brain Research Institute, University of Niigata, Niigata; [9]Comprehensive Epilepsy Center; [10]Department of Pathology, Seirei Hamamatsu General Hospital, Shizuoka; [11]Department of Pediatrics, Toyohashi Municipal Hospital, Toyohashi; [12]Division of Child Neurology, Tottori University Faculty of Medicine, Yonago; [13]Division of Child Neurology, Department of Brain and Neurosciences, Tottori University Faculty of Medicine, Yonago; [14]Department of Pediatrics, Asahikawa Medical University, Asahikawa; [15]Department of Neurology, Nagano Children's Hospital, Azumino; [16]Department of Pediatrics, Kameda Medical Center, Chiba; [17]Department of Pediatrics, Juntendo University Faculty of Medicine, Tokyo; [18]Aichi Welfare Center for Persons with Developmental Disabilities, Kasugai; [19]Department of Pediatrics, Yodogawa Christian Hospital, Osaka; [20]Department of Pediatrics and Neonatology, Nagoya City University Graduate School of Medical Sciences, Nagoya; [21]Department of Pediatric Neurosurgery, Takatsuki General Hospital, Osaka; and [22]Department of Pediatrics, Kitano Hospital, Tazuke Kofukai Medical Research Institute, Osaka, Japan.

Additional supporting information can be found in the online version of this article.

mutations were inherited from asymptomatic parents. Aberrant splicing was demonstrated by reverse transcriptase polymerase chain reaction analyses in 2 patients with splice site mutations.
Interpretation: Our study first confirmed that *COL4A1* mutations are associated with schizencephaly and hemolytic anemia. Based on the finding that *COL4A1* mutations were frequent in patients with porencephaly and schizencephaly, genetic testing for *COL4A1* should be considered for children with these conditions.
ANN NEUROL 2012;00:000–000

Type IV collagens are basement membrane proteins that are expressed in all tissues, including the vasculature. COL4A1 (α1 chain) and COL4A2 (α2 chain) are the most abundant type IV collagens, and form heterotrimers with a 2:1 stoichiometry (α1α1α2).[1] Mutations in *COL4A1* and *COL4A2* cause sporadic and hereditary porencephaly, a neurological disorder characterized by fluid-filled cysts in the brain that often cause hemiplegia or tetraplegia.[2–4] In addition, a variety of clinical phenotypes, including small vessel disease affecting the brain, eyes, and kidneys, are associated with *COL4A1* abnormality[5,6]: neonatal porencephaly and adult stroke,[7] sporadic extensive bilateral porencephaly resembling hydranencephaly,[8] periventricular leukomalacia with intracranial calcification,[9] HANAC (hereditary angiopathy with nephropathy, aneurysm, and muscle cramps) syndrome,[10,11] Axenfeld–Rieger anomaly with leukoencephalopathy, and adult stroke and intracerebral hemorrhage.[12–14] Notably, *COL4A1* mutations were present in 2 patients with muscle–eye–brain/Walker–Warburg syndrome (MEB/WWS), which is characterized by ocular dysgenesis, neuronal migration defects, and congenital muscular dystrophy, suggesting that *COL4A1* is also involved in normal cortical and muscular development in humans.[15] Consistent with this hypothesis, a mouse model of a heterozygous *COL4A1* mutation (*Col4a1*$^{+/\Delta ex40}$) showed ocular dysgenesis, cortical neuronal localization defects, and myopathy, along with cerebral hemorrhage and porencephaly.[2,15] The phenotypic spectrum of *COL4A1* mutations is expanding; however, the whole spectrum of systemic phenotypes and the incidence of *COL4A1* mutations associated with porencephaly has not been systemically examined.

In this study, we screened for *COL4A1* mutations in 61 patients with porencephaly and 10 patients with schizencephaly, which may be similarly caused by disturbed vascular supply leading to cerebral degeneration, but can be distinguished depending on time of insult.[2–4,16,17] *COL4A1* mutations were identified in 10 patients with porencephaly and 5 patients with schizencephaly, who showed a variety of associated findings, including intracranial calcification, focal cortical dysplasia (FCD), ocular abnormalities, pontocerebellar atrophy, myopathy, elevated serum creatine kinase levels, and hemolytic anemia. Our study demonstrated the importance of genetic testing for *COL4A1* in children with porencephaly or schizencephaly.

Patients and Methods

Patients

A total of 61 patients with porencephaly including a previous cohort with porencephaly,[4] and 10 patients with schizencephaly including a patient who also had porencephaly were analyzed for *COL4A1* mutations. Schizencephaly is defined as transmantle clefts bordered by polymicrogyria in adjacent cortex.[18] The clefts extended through the entire hemisphere, from the ependymal lining of the lateral ventricles to the pial covering of the cortex.[19] The clefts are further divided into those with closed lips and those with open lips. In the clefts with closed lips, the walls affix each other directly, obliterating the cerebrospinal fluid space within the cleft at that point.[20] *COL4A2* mutations were negative for these patients. Genomic DNA was isolated from blood leukocytes according to standard methods, and amplified using an illustra GenomiPhi V2 DNA Amplification Kit (GE Healthcare, Buckinghamshire, UK). The DNA of familial members of patient 6 was isolated from saliva samples using Oragene (DNA Genotek, Kanata, Ontario, Canada). Experimental protocols were approved by the committee for ethical issues at Yokohama City University School of Medicine. All patients were investigated in agreement with the requirements of Japanese regulations.

Mutation Analysis

Exons 1 to 52, covering the entire *COL4A1* coding region, were examined by high-resolution melting (HRM) curve analysis. Samples showing an aberrant melting curve pattern in the HRM analysis were sequenced. Polymerase chain reaction (PCR) primers and conditions are shown in Supplementary Table S1. All novel mutations were verified using original genomic DNA, and screened in 200 Japanese normal controls by HRM analysis. For the family showing de novo mutations, parentage was confirmed by microsatellite analysis, as previously described.[21] Biological parents were confirmed if >4 informative markers were compatible and other markers showed no discrepancy.

Reverse Transcriptase-PCR

Reverse transcriptase (RT)-PCR using total RNA extracted from lymphoblastoid cell lines (LCL) was performed essentially as previously described.[22] Briefly, total RNA was extracted using RNeasy Plus MiniKit (Qiagen, Tokyo, Japan) from LCL with or without 30μM cycloheximide (CHX; Sigma, Tokyo, Japan) incubation for 4 hours. Four micrograms total RNA was subjected to reverse transcription, and 2μl cDNA was used for PCR. Primer sequences are ex20-F (5′-CCCAAAAGGTTTCC CAGGACTACCA-3′) and ex22-R (5′-GTCCGGGCTGACAT TCCACAATTC-3′; for patient 4); and ex22-F (5′-GAATTC-CAGGGCAGCCAGGATTTAT-3′) and ex24-R (5′-CATCTCT GCCAGGCAAACCTCTGT-3′; for patient 7). DNA of each

PCR band was purified by QIAEXII Gel extraction kit (Qiagen; for patient 4) and E.Z.N.A. poly-Gel DNA Extraction kit (Omega Bio-Tek, Norcross, GA; for patient 7), respectively.

Results

Mutation and RT-PCR analysis

COL4A1 abnormalities were identified in 15 patients (Fig 1 and Table). Nine mutations occurred at highly conserved Gly residues in the Gly-X-Y repeat of the collagen triple helical domain. Interestingly, a missense mutation (c.4843G>A [p.Glu1615Lys]) at an evolutionary conserved amino acid and a nonsense mutation (c.4887C>A [p.Tyr1629X]) were found in the carboxy-terminal noncollagenous (NC1) domain. The other 4 mutations include a frameshift mutation (c.2931dupT [p.Gly978TrpfsX15]) and 3 splice site mutations (c.1121-2dupA, c.1382-1G>C, and c.1990+1G>A). None of these mutations was present in 200 Japanese normal controls, and Web-based prediction tools suggested that these mutations are pathogenic (Supplementary Table S2). The c.2842G>A (patient 1), c.3976G>A (patient 2), c.4887C>A (patient 8), c.2689G>A (patient 13), and c.1990+1G>A (patient 14) mutations occurred de novo. The c.3995G>A mutation (patient 3) was not found in the mother's DNA (the father's DNA was unavailable). The c.1121-2dupA (patient 4) and c.2931dupT (patient 6) mutations were found in the asymptomatic fathers. c.1963G>A (patient 10) was found in familial members affected with porencephaly as well as asymptomatic carriers, suggesting incomplete penetrance of the mutation (Supplementary Fig S1). The remaining patients' parental DNA was unavailable.

To examine the mutational effects of the 2 splice acceptor site mutations (c.1121-2dupA and c.1382-1G>C), RT-PCR and sequencing were performed (see Fig 1). c.1121-2dupA caused the deletion of exon 21 from the wild-type *COL4A1* mRNA, resulting in an in-frame 55-amino acid deletion (p.Gly374_Asn429delinsAsp). The effect of c.1382-1G>C was more complicated. There were 3 PCR products amplified from LCL treated with CHX, which inhibits nonsense-mediated mRNA decay (NMD). The middle band corresponded to the wild-type allele. The sequence of the lower mutant band showed a 33bp insertion of intron 22 and an 84bp deletion of all of exon 23 from the use of cryptic splice acceptor and donor sites within intron 22. The change of amino acid sequence from this mutant transcript was a deletion of 29 amino acids and an insertion of 12 amino acids (p.Gly461_Gly489delinsValHisCysGlyAspPheTrpSerHisValThrArg). The upper band was only observed in CHX-treated LCL, but was not evident in the untreated LCL, suggesting that this mutant transcript may undergo NMD. Sequencing of the upper band showed a 61bp insertion of intron 22 from the use of a cryptic splice acceptor site within intron 22, as mentioned above. The product of this mutant transcript leads to a frameshift, creating a premature stop codon (p.Gly461ValfsX31), which is consistent with degradation of the mutant transcript by NMD.

Clinical Features

The clinical information for individuals with *COL4A1* mutations is summarized in the Table, and their representative brain images are shown in Figure 2 and Supplementary Fig S2. *COL4A1* mutations were identified in 10 of 61 patients with porencephaly (16.4%). Of note, *COL4A1* mutations were identified in 5 of 10 patients with schizencephaly (50.0%), revealing a novel association between *COL4A1* mutations and schizencephaly. Thirteen patients were born at term, and 2 patients (patients 1 and 12) were born at preterm. Their body weight was normal at birth except for 5 patients (patients 3, 4, 9, 12, and 15) who were below −2.0 standard deviations. The occipitofrontal circumference was available in 12 patients, and 6 patients (patients 2, 3, 6, 13, 14, and 15) were below −2.0 standard deviations. Two patients (patients 11 and 12) were confirmed to have an antenatal hemorrhage as previously reported.[23,24] Among associated findings with *COL4A1* mutations, a patient showed FCD that was histologically demonstrated (Fig 3A–F). In addition, hemolytic anemia was found in 5 of 15 patients, suggesting that hemolytic anemia may be a novel feature associated with *COL4A1* mutation. Pontocerebellar atrophy along with severe bilateral porencephaly was observed in 2 patients, and a patient showed cerebellar hypoplasia. Previously reported magnetic resonance imaging and systemic findings associated with *COL4A1* mutations were also observed, including intracranial calcification (7 of 15), myopathy (1 of 15; see Fig 3G, H), ocular abnormalities (4 of 15), and elevated serum creatine kinase levels (6 of 15), confirming that these features are useful signs for *COL4A1* testing. Case reports are available in the Supplementary Data.

Discussion

We found a total of 15 novel mutations in this study. Nine mutations occurred at highly conserved Gly residues in the Gly-X-Y repeat of the collagen triple helical domain, suggesting that these mutations may alter the collagen IV $\alpha1\alpha1\alpha2$ heterotrimers.[1,25] We reported for the first time 2 mutations (a nonsense and a missense change) in the NC1 domain. The nonsense mutation

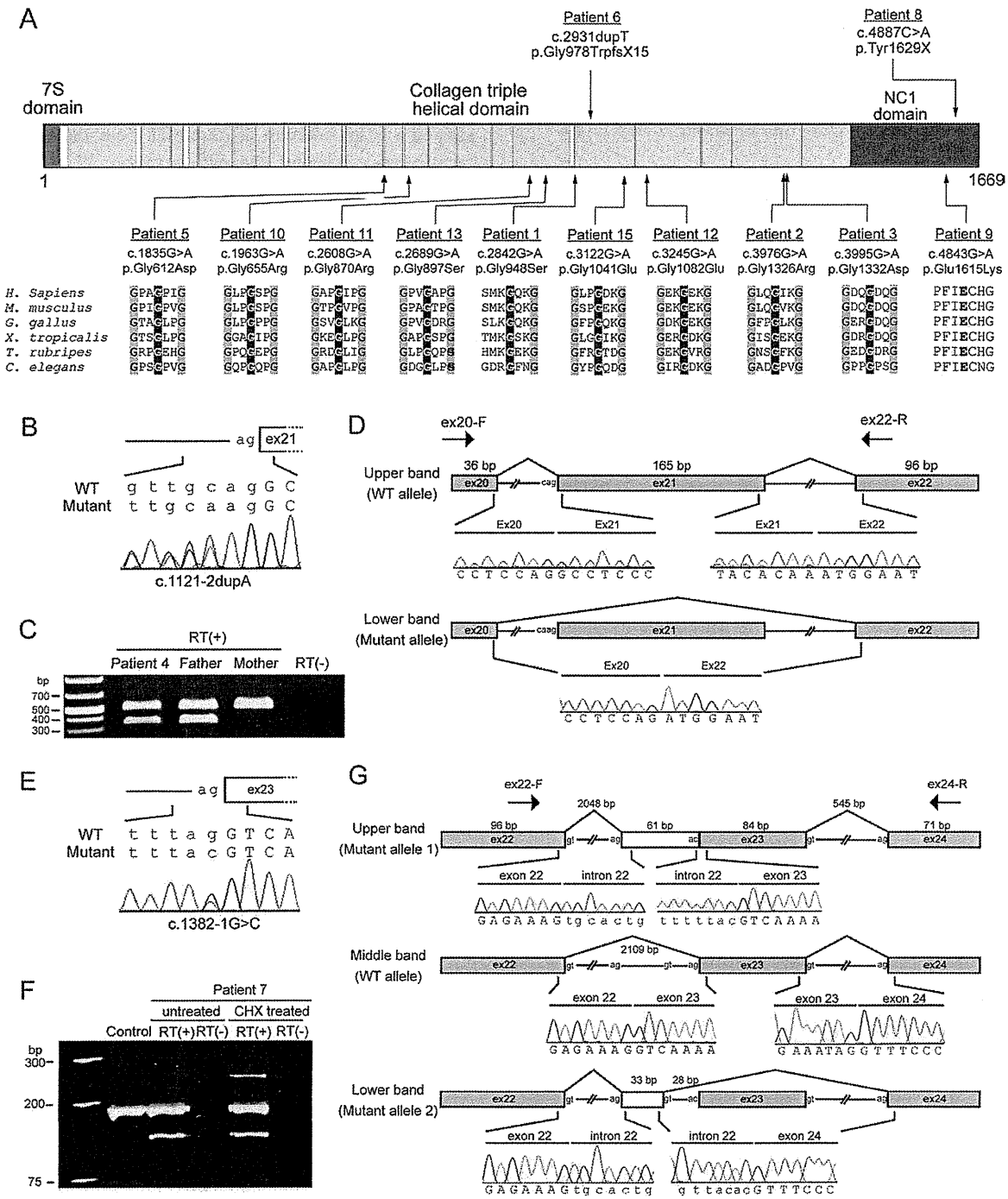

FIGURE 1: ***COL4A1*** **mutations in patients with porencephaly or schizencephaly. (A) Functional domains of COL4A1 protein. The locations of 12 mutations, including 10 missense mutations (bottom), a nonsense mutation, and a frameshift mutation (top) are indicated by arrows. The 7S domain is highlighted with blue and the NC1 domain with red. Gly-X-Y repeats within the collagen triple helical domain are highlighted with yellow. All of the missense mutations occurred at evolutionary conserved amino acids. The positions of the conserved Gly residues in the Gly-X-Y repeats are highlighted in gray. Homologous sequences were aligned using CLUSTALW (http://www.genome.jp/tools/clustalw/). (B) The c.1121-2dupA mutation in intron 20 is colored red. Sequences of exons and introns are presented in upper and lower cases, respectively. (C) Reverse transcriptase (RT)-polymerase chain reaction (PCR) analysis of patient 4 and his parents. (D) Schematic presentation of the wild-type (WT; upper) and mutant (lower) transcripts and primers used for analysis. A single band (500bp), corresponding to the WT allele, was amplified using the mother's cDNA template. Conversely, a lower band was detected from the cDNA from the patient and his father. In the mutant transcript, the 165bp exon 21 was deleted. Sequences of exons and introns are presented in upper and lower cases, respectively. (E) The c.1382-1G>C mutation in intron 22 is colored red. (F) RT-PCR analysis of patient 7 and a control. (G) Schematic representation of the WT and mutant transcripts, and primers used for analysis. A single band (183bp), corresponding to the WT allele, was amplified using a control cDNA template. Conversely, upper and lower bands were detected from the patient's cDNA. The upper band (244bp), which was observed only in cycloheximide (CHX)-treated cells, had a 61bp insertion of intron 22 sequences, leading to a frameshift. Absence of the upper band in untreated lymphoblastoid cell lines strongly suggests that the mutant transcript may undergo nonsense-mediated mRNA decay. The lower band had a 33bp insertion of intron 22 and 84bp deletion of the whole of exon 23, leading to an in-frame 51bp deletion.**

TABLE: Clinical features of patients with *COL4A1* mutations

Cases	Age	Sex	Mutation	Inheritance	Brain MRI/ CT findings	CP	Epi	Ocular features	Family history	ID	Hyper-CK	Other
1	14y	M	c.2842G>A (p.Gly948Ser)	de novo	Bilateral POCE, calcification, hemosiderin deposition	Q	+	-	-	+	-	
2	18m	M	c.3976G>A (p.Gly1326Arg)	de novo	Bilateral SCZ, calcification, hemosiderin deposition	Q	+	-	-	+	-	
3	15m	M	c.3995G>A (p.Gly1332Asp)	Absent in mother	Unilateral SCZ, calcification, hemosiderin deposition	H	+	-	-	+	-	
4	6y	M	c.1121-2dupA[1)]	Paternal	Unilateral POCE	H	+	-	-	+	-	FCD
5	2m	F	c.1835G>A (p.Gly612Asp)	ND	Bilateral SCZ, calcification, thin CC, thin brain stem, cerebellar atrophy, absence of SP, hemosiderin deposition, multicystic encephalomalacia,	Q	+	Optic nerve hypoplasia	-	+	+	HA
6	7y	M	c.2931dupT (p.Gly978TrpfsX15)	Paternal	Unilateral POCE	H	+	-	-	+	+	
7	12y	F	c.1382-1G>C[2)]	ND	Unilateral POCE	H	+	-	-	+	+	Myopathy
8	10y	M	c.4887C>A (p.Tyr1629X)	de novo	Unilateral POCE	H	+	-	Hematuria	+	-	
9	3m	F	c.4843G>A (p.Glu1615Lys)	ND	Bilateral POCE, calcification, hypoplastic CC, hemosiderin deposition, thin	Q	+	Microphthalmia Corneal opacity	-	+	-	VSD, HA

TABLE (Continued)

Cases	Age	Sex	Mutation	Inheritance	Brain MRI/ CT findings	CP	Epi	Ocular features	Family history	ID	Hyper-CK	Other
					brain stem, cerebellar atrophy, multicystic encephalomalacia							
10	2y7m	F	c.1963G>A (p.Gly655Arg)	Paternal[3)]	Bilateral POCE	Q	+	-	POCE, Epi	+	-	-
11	1y	F	c.2608G>A (p.Gly870Arg)	ND	Unilateral POCE, calcification	Q	+	Congenital cataract	-	+	-	-
12	1y5m	M	c.3245G>A (p.Gly1082Glu)	ND	Unilateral SCZ with bilateral POCE, calcification, cerebellar hypoplasia	T	+	Congenital cataract	-	+	-	HA, Hematuria
13	3y7m	M	c.2689G>A (p.Gly897Ser)	de novo	Unilateral POCE	Q	+	-	-	+	+	-
14	9m	F	c.1990+1G>A	de novo	Unilateral POCE, hemosiderin deposition	Q	+	-	-	+	+	HA, Hematuria
15	2y	F	c.3122G>A (p.Gly1041Glu)	ND	Unilateral SCZ, hemosiderin deposition	Q	+	-	-	+	+	HA

1) p.Gly374_Asn429delinsAsp change was predicted by mRNA analysis
2) Two alternative protein chages were predicted by mRNA analysis: p.Gly461_Gly489delinsValHisCysGlyAspPheTrpSerHisValThrArg and p.Gly461ValfsX31. y, years; m, months; M, male; F, female; ND, Not determined; POCE, porencephaly, SCZ, schizencephaly; CC, corpus callosum; SP, septum pellucidum; CP, cerebral palsy; H, hemiplegia; T, Triplegia; Q, quadriplegia; Epi, epilepsy; ID, intellectual disability; CK, creatine kinase; FCD, Focal cortical dysplasia; HA, Hemolytic anemia; VSD, ventricular septal defect
3) Co-segregation of the p.Gly655Arg mutation with porencephaly was confirmed.

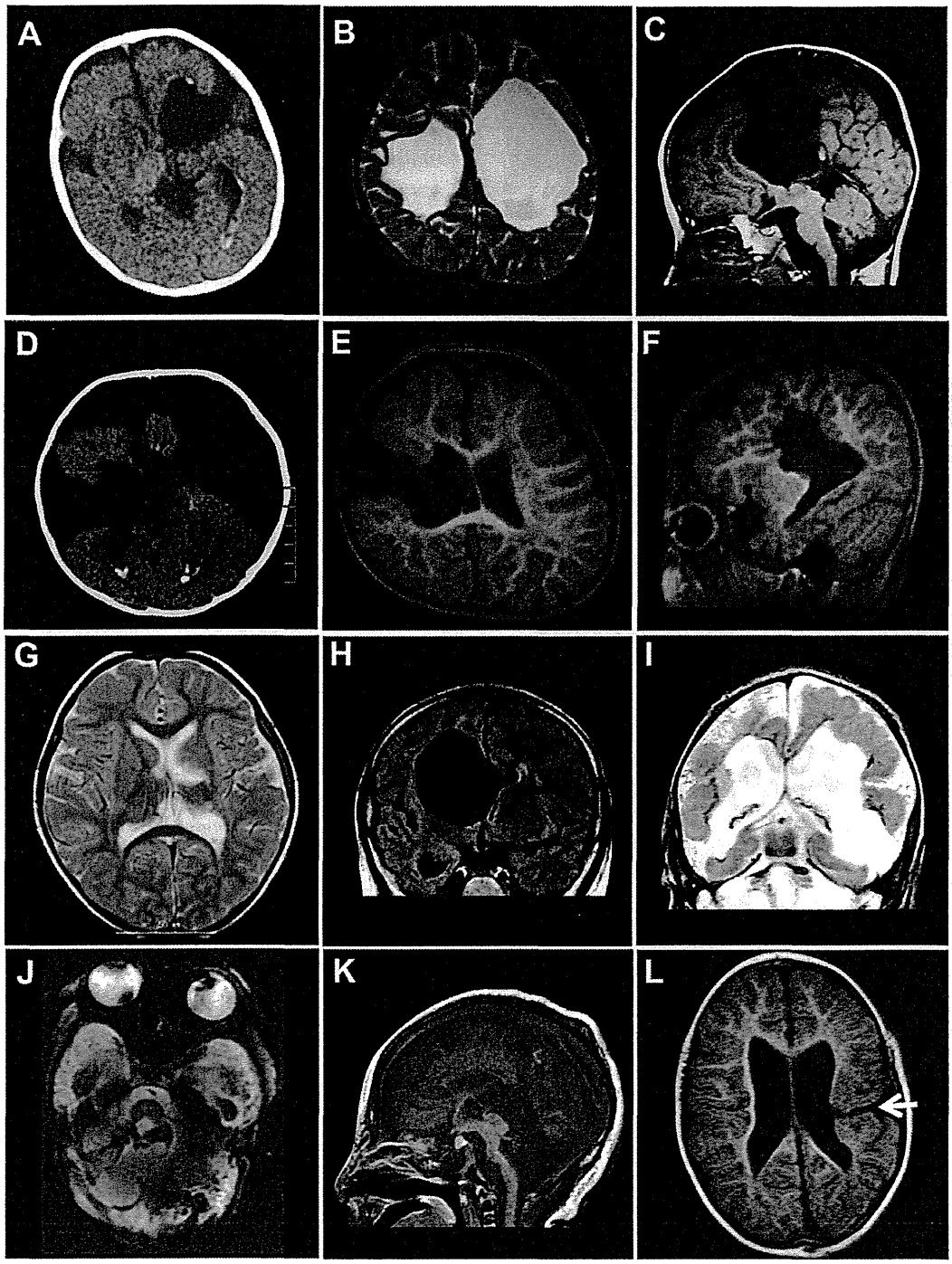

FIGURE 2: Computed tomography (CT) scan (A, D) and magnetic resonance imaging (MRI; B, C, E–L) of patients with *COL4A1* mutations. (A–C) Images of patient 1. (A) The CT scan shows calcification along with the dilated lateral ventricular wall. (B) T2-weighted and (C) T1-weighted images (WIs) at 5 years of age showing bilateral porencephaly. (D) The CT image of patient 2 with schizencephaly shows calcification of the lateral ventricular wall and brain parenchyma. (E, F) T1-WIs of patient 3 show unilateral schizencephaly at 15 months of age. (G) T2-WI of patient 4 at 3 years of age shows parenchymal defect of the left thalamus and basal ganglia due to subependymal hemorrhage. (H) Fluid-attenuated inversion recovery image of patient 7 at 6 years of age showing unilateral porencephaly. (I) T2-WI, (J) T2*-weighted gradient-echo image (WGRE), and (K) T1-WI of patient 9. (I) The MRI at 2 months of age shows bilateral porencephaly with low-intensity lesions along with a deformed ventricular wall, which has hemosiderin deposition and calcification. (J) T2*-WGRE showing hemosiderin deposition in the atrophic cerebellum. The atrophic pontocerebellar structures are also shown in (K). (L) T1-WI of patient 15 showed schizencephaly in the left hemisphere at 2 years of age.

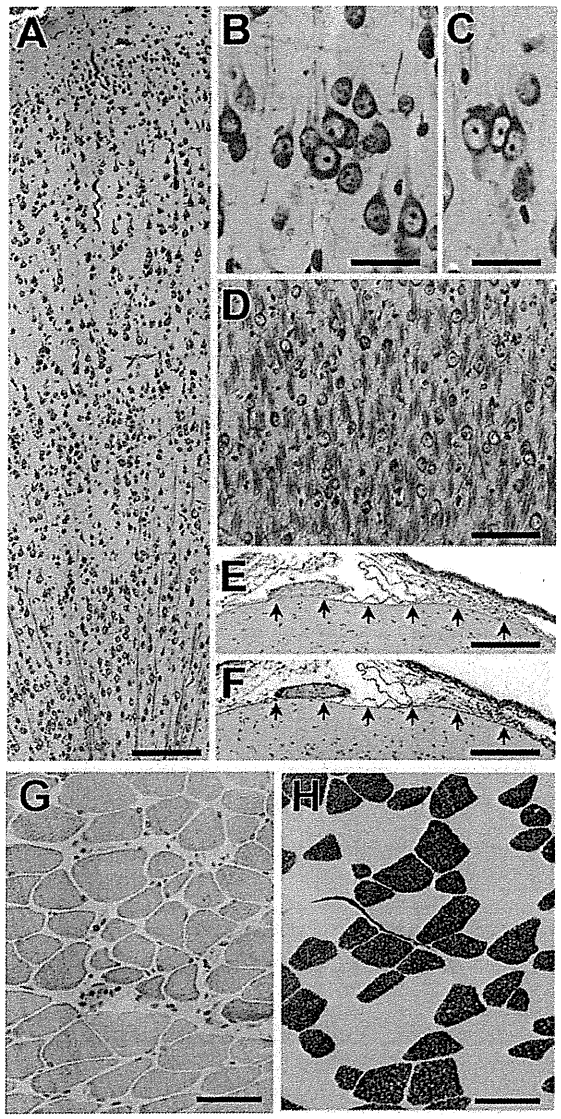

FIGURE 3: Histopathological features of the resected frontal tissue of patient 4 (A–F) and biopsied rectus abdominis muscle of patient 7 (G, H). (A) Low-magnification view of the cortex showing architectural abnormalities. (B, C) Two examples of neuronal clustering. (D) Many neurons scattered within the subcortical white matter. (E, F) Two serial sections demonstrating the superficial layer of the cortex. Note that the basal lamina of the pia mater (*arrows* in each panel) is continuously labeled with antibodies against collagen type IV (E) and laminin (F). (A–D) Klüver–Barrera stain. (E, F) Immunostained and then counterstained with hematoxylin. (G) Hematoxylin and eosin staining showing variation in fiber size, slightly increased endomysial connective tissue, and internal nuclei. (H) Adenosine triphosphatase (pH 4.5) staining showing type 2B fiber deficiency. There was no increase in number of type 2C fibers. Scale bars indicate 175μm (A, E, F), 30μm (B, C), 80μm (D), and 30μm (G, H).

would cause a truncation of the NC1 domain rather than mRNA degradation by NMD as the mutation was located within 50bp of the exon–intron boundary of the second to last exon (exon 51).[26] The NC1 domains are the sites for molecular recognition through which the stoichiometry of chains in the assembly of triple-helical formation is directed[1]; therefore, these 2 mutations may alter the assembly of the collagen IV $\alpha1\alpha1\alpha2$ heterotrimers. In addition, the effect of 2 splice site mutations was examined using LCL, suggesting that in-frame deletion/insertion mutant protein should be produced. Thus, it is highly likely that impairment of the collagen IV $\alpha1\alpha1\alpha2$ heterotrimer assembly caused by mutant $\alpha1$ chain is a common pathological mechanism of *COL4A1* mutations. The c.2931dupT mutation found in patient 6 and his father might cause severe truncation of COL4A1 protein. It is possible that the truncation of COL4A1 protein can also impair $\alpha1\alpha1\alpha2$ heterotrimer assembly similar to substitutions of conserved Gly residues in the Gly-X-Y repeat. Alternatively, the mutant transcript might undergo NMD, and haploinsufficiency of *COL4A1* might cause a weakness of basement membrane. Biological analysis using patients' cells will clarify these possibilities.

COL4A1 mutations in schizencephaly were first demonstrated in this study. Schizencephaly was used by Yakovlev and Wadsworth in 1946 to describe true clefts formed in the brain as a result of failure of development of the cortical mantle in the zones of cleavage of the primary cerebral fissures.[19] Schizencephaly is differentiated from clefts in the central mantle that arise as the result of a destruction of the cerebral tissues, which they called encephalocrastic porencephalies, now known simply as porencephaly.[19] Schizencephaly has been understood as a neuronal migration disorder, because the clefts are lined by abnormal gray matter, described as polymicrogyria. Conversely, porencephaly is understood to be a postmigration accident resulting in lesions, without gray matter lining the clefts or an associated malformation of cortical development. It has been suggested that both schizencephaly and porencephaly are caused by encephaloclastic regions, and can be distinguished depending on time of insult.[16,17] The present study clearly demonstrated that *COL4A1* mutations caused both porencephaly and schizencephaly, supporting the same pathological mechanism for these 2 conditions.

The genes responsible for FCD have been elusive, despite extensive investigation. The pathological features of the cortical tubers of tuberous sclerosis (TSC) may be indistinguishable from those of FCD. Apart from FCD due to TSC, there is only 1 gene that may explain the genetic basis of FCD, where a homozygous mutation in *CNTNAP2* has been identified in Amish children with FCD, macrocephaly, and intractable seizures.[27] Surprisingly, the present study discovered a patient with FCD

and porencephaly, in whom aberrant splicing was demonstrated and FCD1A was pathologically confirmed using resected brain tissues. A recent report revealed *COL4A1* mutations in 2 patients with MEB/WWS showing cobblestone lissencephaly,[15] and abnormal cortical development has been observed in mouse models of *COL4A1* mutations.[15,28] Thus, it is possible that *COL4A1* mutations are involved in cerebral cortical malformations, including FCD. Identification of a greater number of cases is required to confirm the association between *COL4A1* mutations and cortical malformations in humans.

In a few children, the sequelae were much more severe than would be expected on the basis of their imaging findings. This is of importance when counseling parents with regard to prediction of neurodevelopmental outcome.

Two patients with *COL4A1* mutations showed intracranial calcification, pontocerebellar atrophy, ocular abnormalities, and hemolytic anemia associated with severe bilateral porencephaly (patient 9) or schizencephaly (patient 5). Severe hemorrhagic destructive lesions in the cerebrum were observed in these patients, and T2* images also showed hemorrhage in the cerebellum, which may have resulted in a thin brainstem and severe cerebellar atrophy. Thus, these 2 patients could be considered as the most severe manifestations affecting the developing brain and eyes. A common feature of the 2 patients is hemolytic anemia of an unknown cause, which required frequent blood transfusions. Five of 15 patients with *COL4A1* mutations showed hemolytic anemia. Interestingly, 2 reports have demonstrated that mouse *Col4a1* mutants showed a significant reduction in red blood cell (RBC) number and hematocrit.[28,29] Given that *Col4a1* mutations lead to hemorrhage, chronic hemorrhage is possibly involved in RBC loss. Alternatively, the *Col4a1* mutation may directly affect blood progenitor cells, as they transmigrate across basement membranes before entering the peripheral blood.[30] Hemolytic anemia in patients with *COL4A1* mutations would imply the latter explanation. Further studies are required to clarify how *COL4A1*/*Col4a1* mutations are involved in anemia.

In summary, we found 15 mutations in *COL4A1* among 71 patients with porencephaly or schizencephaly, showing an unexpectedly high percentage of mutations (about 21%) in these patients. Fourteen patients with *COL4A1* mutations had no family history of cerebral palsy. The 15 patients with *COL4A1* mutations showed a variety of phenotypes, further expanding the possible clinical spectrum of *COL4A1* mutations to include schizencephaly, FCD, pontocerebellar atrophy, and hemolytic anemia. Genetic testing for *COL4A1* should be recommended for children with porencephaly and schizencephaly.

Acknowledgment

This work was supported by research grants from the Ministry of Health, Labor, and Welfare (K.H., M.K., H.O., N.Mi., N.Ma., H.S.), Japan Science and Technology Agency (N.Ma.), and Strategic Research Program for Brain Sciences (11105137 to N.Ma.), a Grant-in-Aid for Scientific Research on Innovative Areas (Foundation of Synapse and Neurocircuit Pathology) from the Ministry of Education, Culture, Sports, Science, and Technology of Japan (11001956 to N.Ma.), a Grant-in-Aid for Scientific Research from the Japan Society for the Promotion of Science (H.O., N.Ma.), a Grant-in-Aid for Young Scientists from the Japan Society for the Promotion of Science (H.D., N.Mi., H.S.), and a grant from the Takeda Science Foundation (N.Mi., N.Ma.). This work was performed at the Advanced Medical Research Center, Yokohama City University, Japan.

We thank the patients and their family members for their participation in this study.

Authorship

Y.Y. and K.H. contributed equally to this work.

Potential Conflicts of Interest

Nothing to report.

References

1. Khoshnoodi J, Pedchenko V, Hudson BG. Mammalian collagen IV. Microsc Res Tech 2008;71:357–370.
2. Gould DB, Phalan FC, Breedveld GJ, et al. Mutations in Col4a1 cause perinatal cerebral hemorrhage and porencephaly. Science 2005;308:1167–1171.
3. Breedveld G, de Coo IF, Lequin MH, et al. Novel mutations in three families confirm a major role of COL4A1 in hereditary porencephaly. J Med Genet 2006;43:490–495.
4. Yoneda Y, Haginoya K, Arai H, et al. De novo and inherited mutations in COL4A2, encoding the type IV collagen alpha2 chain cause porencephaly. Am J Hum Genet 2012;90:86–90.
5. Vahedi K, Alamowitch S. Clinical spectrum of type IV collagen (COL4A1) mutations: a novel genetic multisystem disease. Curr Opin Neurol 2011;24:63–68.
6. Lanfranconi S, Markus HS. COL4A1 mutations as a monogenic cause of cerebral small vessel disease: a systematic review. Stroke 2010;41:e513–e518.
7. van der Knaap MS, Smit LM, Barkhof F, et al. Neonatal porencephaly and adult stroke related to mutations in collagen IV A1. Ann Neurol 2006;59:504–511.
8. Meuwissen ME, de Vries LS, Verbeek HA, et al. Sporadic COL4A1 mutations with extensive prenatal porencephaly resembling hydranencephaly. Neurology 2011;76:844–846.

9. Livingston J, Doherty D, Orcesi S, et al. COL4A1 Mutations associated with a characteristic pattern of intracranial calcification. Neuropediatrics 2011;42:227–233.
10. Plaisier E, Gribouval O, Alamowitch S, et al. COL4A1 mutations and hereditary angiopathy, nephropathy, aneurysms, and muscle cramps. N Engl J Med 2007;357:2687–2695.
11. Alamowitch S, Plaisier E, Favrole P, et al. Cerebrovascular disease related to COL4A1 mutations in HANAC syndrome. Neurology 2009;73:1873–1882.
12. Coutts SB, Matysiak-Scholze U, Kohlhase J, Innes AM. Intracerebral hemorrhage in a young man. CMAJ 2011;183:E61–E64.
13. Sibon I, Coupry I, Menegon P, et al. COL4A1 mutation in Axenfeld-Rieger anomaly with leukoencephalopathy and stroke. Ann Neurol 2007;62:177–184.
14. Weng YC, Sonni A, Labelle-Dumais C, et al. COL4A1 mutations in patients with sporadic late-onset intracerebral hemorrhage. Ann Neurol 2012;71:470–477.
15. Labelle-Dumais C, Dilworth DJ, Harrington EP, et al. COL4A1 mutations cause ocular dysgenesis, neuronal localization defects, and myopathy in mice and Walker-Warburg syndrome in humans. PLoS Genet 2011;7:e1002062.
16. Friede R. Porencephaly, hydranencephaly, multicystic encephalopathy. In: Developmental neuropathology. 2nd ed. Berlin, Germany: Springer-Verlag, 1989:28–43.
17. Govaert P. Prenatal stroke. Semin Fetal Neonatal Med 2009;14: 250–266.
18. Barkovich AJ, Guerrini R, Kuzniecky RI, et al. A developmental and genetic classification for malformations of cortical development: update 2012. Brain 2012;135:1348–1369.
19. Yakovlev PI, Wadsworth RC. Schizencephalies; a study of the congenital clefts in the cerebral mantle; clefts with fused lips. J Neuropathol Exp Neurol 1946;5:116–130.
20. Barkovich AJ, Kjos BO. Schizencephaly: correlation of clinical findings with MR characteristics. AJNR Am J Neuroradiol 1992;13: 85–94.
21. Saitsu H, Kato M, Mizuguchi T, et al. De novo mutations in the gene encoding STXBP1 (MUNC18–1) cause early infantile epileptic encephalopathy. Nat Genet 2008;40:782–788.
22. Saitsu H, Kato M, Okada I, et al. STXBP1 mutations in early infantile epileptic encephalopathy with suppression-burst pattern. Epilepsia 2010;51:2397–2405.
23. Lichtenbelt KD, Pistorius LR, De Tollenaer SM, et al. Prenatal genetic confirmation of a COL4A1 mutation presenting with sonographic fetal intracranial hemorrhage. Ultrasound Obstet Gynecol 2012;39:726–727.
24. de Vries LS, Koopman C, Groenendaal F, et al. COL4A1 mutation in two preterm siblings with antenatal onset of parenchymal hemorrhage. Ann Neurol 2009;65:12–18.
25. Engel J, Prockop DJ. The zipper-like folding of collagen triple helices and the effects of mutations that disrupt the zipper. Annu Rev Biophys Biophys Chem 1991;20:137–152.
26. Nagy E, Maquat LE. A rule for termination-codon position within intron-containing genes: when nonsense affects RNA abundance. Trends Biochem Sci 1998;23:198–199.
27. Strauss KA, Puffenberger EG, Huentelman MJ, et al. Recessive symptomatic focal epilepsy and mutant contactin-associated protein-like 2. N Engl J Med 2006;354:1370–1377.
28. Favor J, Gloeckner CJ, Janik D, et al. Type IV procollagen missense mutations associated with defects of the eye, vascular stability, the brain, kidney function and embryonic or postnatal viability in the mouse, Mus musculus: an extension of the Col4a1 allelic series and the identification of the first two Col4a2 mutant alleles. Genetics 2007;175:725–736.
29. Van Agtmael T, Bailey MA, Schlotzer-Schrehardt U, et al. Col4a1 mutation in mice causes defects in vascular function and low blood pressure associated with reduced red blood cell volume. Hum Mol Genet 2010;19:1119–1128.
30. Janowska-Wieczorek A, Marquez LA, Nabholtz JM, et al. Growth factors and cytokines upregulate gelatinase expression in bone marrow CD34(+) cells and their transmigration through reconstituted basement membrane. Blood 1999;93:3379–3390

Reply

Aron S. Buchman, MD,[1,2] Joshua M. Shulman, MD, PhD,[3,4] Sue E. Leurgans, PhD,[1,2] Julie A. Schneider, MD, MS,[1,2,5] and David A. Bennett, MD[1,2]

We thank Drs Jellinger and Attems for their interest in our study. In agreement with prior reports, we found that Parkinson disease (PD) pathology, including nigral neuronal loss and Lewy body pathology, is common in older adults without PD. Furthermore, we provide evidence that PD nigral pathology is related to parkinsonian motor signs in persons without a clinical diagnosis of PD.[1] This contrasts with prior studies of incidental Lewy body disease, which found associations with subtle electrophysiologic changes but not with overt motor signs.[2] Interestingly, in the current study, we also found that Alzheimer disease (AD) and cerebrovascular pathology showed independent associations with the severity of parkinsonian motor signs.[1] As requested, the correlations among these common brain pathologies are included in the accompanying Table. It is interesting that Dr Attems and colleagues did not find an association of nigral pathology or cerebrovascular disease with parkinsonian signs among persons with AD.[3] We and others have reported such associations.[4–6] Overall, the findings in the current study have important public health implications. They suggest that mild parkinsonian signs, reported in up to 50% of older adults by age 85 years and associated with significant morbidity and mortality, may be caused by a range of pathologies including PD pathology, AD, and cerebrovascular pathologies. These data underscore the need for more sensitive clinical measures and biomarkers that can detect and differentiate the various neuropathologies underlying the development of parkinsonian signs in old age.

Potential Conflicts of Interest

Nothing to report.

[1]Rush Alzheimer's Disease Center and [2]Department of Neurological Sciences, Rush University Medical Center, Chicago, IL, [3]Department of Neurology, Brigham and Women's Hospital, Boston, MA, [4]Department of Neurology, Harvard Medical School, Boston, MA, and [5]Department of Pathology (Neuropathology), Rush University Medical Center, Chicago, IL

References

1. Buchman AS, Shulman JM, Nag S, et al. Nigral pathology and parkinsonian signs in elders without Parkinson disease. Ann Neurol 2012;71:258–266.
2. Caviness JN. Presymptomatic Parkinson's disease: the Arizona experience. Parkinsonism Relat Disord 2012;18(suppl 1):S203–S206.
3. Attems J, Quass M, Jellinger K. Tau and α-synuclein brainstem pathology in Alzheimer disease: relation with extrapyramidal signs. Acta Neuropathol 2007;113:53–62.
4. Burns JM, Galvin JE, Roe CM, et al. The pathology of the substantia nigra in Alzheimer disease with extrapyramidal signs. Neurology 2005;64:1397–1403.
5. Schneider JA, Li JL, Li Y, et al. Substantia nigra tangles are related to gait impairment in older persons. Ann Neurol 2006;59:166–173.
6. Buchman AS, Leurgans SE, Nag S, et al. Cerebrovascular disease pathology and parkinsonian signs in old age. Stroke 2011;42:3183–3189.

DOI: 10.1002/ana.23639

Whole Exome Sequencing Identifies *KCNQ2* Mutations in Ohtahara Syndrome

Hirotomo Saitsu, MD, PhD,[1] Mitsuhiro Kato, MD, PhD,[2] Ayaka Koide, MD, PhD,[3] Tomohide Goto, MD, PhD,[3] Takako Fujita, MD,[4] Kiyomi Nishiyama, PhD,[1] Yoshinori Tsurusaki, PhD,[1] Hiroshi Doi, MD, PhD,[1] Noriko Miyake, MD, PhD,[1] Kiyoshi Hayasaka, MD, PhD,[2] and Naomichi Matsumoto, MD, PhD[1]

Recently, Weckhuysen et al revealed that *KCNQ2* mutations are involved in a substantial proportion of patients with a neonatal epileptic encephalopathy.[1] Some cases showed a suppression–burst pattern on electroencephalogram (EEG), tonic seizures, and profound intellectual disability, resembling Ohtahara syndrome (OS). By whole exome sequencing analysis of 12

TABLE: Intercorrelation of Postmortem Indices

Index	Macroinfarcts	Microinfarcts	Arteriolosclerosis	AD Pathology	Nigral Lewy Bodies
Nigral neuronal loss	0.07, 0.068	0.02, 0.628	0.13, <0.001	0.14, <0.001	0.38, <0.001
Macroinfarcts	—	0.39, 0.056	0.26, <0.001	0.09, 0.017	−0.063, 0.072
Microinfarcts		—	0.15, <0.001	0.04, 0.315	−0.10, 0.075
Arteriolosclerosis			—	0.03, 0.385	0.03, 0.491
AD pathology				—	0.07, 0.052

Based on Spearman or tetrachoric correlation and *p* value.

TABLE: Summary of the Clinical Features of Subjects with *KCNQ2* Mutations

Case #	Mutation	Sex	Age	Age at Onset, Days	Initial Symptoms	Initial Epileptic Attacks	Initial EEG	Age at Onset of Spasms, Days	Age at Onset of SB Pattern, Days	Response to Therapy	Other Drugs Used, but Ineffective	Development	Neurological Examination	Involuntary Movement
1469	c.1010C>G (p.A337G) de novo	M	7 years	7	Vomiting	7 days, tonic seizure	SB	—	22	Seizure free and SB on EEG, disappeared after high-dose PB, CPS since age 5 years	B6, ZNS	No meaningful words, able to crawl, stand with support	Severe MR, no pyramidal signs	No
1654	c.341C>T (p.T114I) de novo	F	7 years	0	Tremor of the upper extremities	2 days, generalized convulsion with cyanosis	SB	—	2	Seizure free after ZNS, CPS since age 5 years	B6, CZP, PHT	DQ 10, bed-ridden, smiling	Profound MR, spastic quadriplegia	No
1754	c.794C>T (p.A265V) de novo	M	3 months	1	Apneic spell	1 days, tonic spasms with right opsoclonuslike movement	SB	1	2	Intractable	B6, ZNS, VPA, CZP, CBZ	Delayed, no eye pursuit	Unknown	Myoclonus at the bilateral upper extremities

B6 = vitamin B6; CBZ = carbamazepine; CPS = complex partial seizures; CZP = clonazepam; DQ = developmental quotient; EEG = electroencephalogram; MR = mental retardation; PB = phenobarbital; PHT = phenytoin; SB = suppression–burst; VPA = valproic acid; ZNS = zonisamide.

patients with OS, we found 3 missense mutations in *KCNQ2* (25%): c.341C>T (p.T114I), c.1010C>G (p.A337G), and c.794C>T (p.A265V) in 3 patients. All 3 patients showed initial seizures early in the neonatal period and a characteristic suppression–burst pattern on EEG, leading to diagnosis as OS (Table). Seizures were temporarily well controlled in 2 patients. Consistent with Weckhuysen's report, in which 6 of 8 mutations arose de novo, the 3 mutations in our series are de novo changes. Thus, it is likely that de novo *KCNQ2* mutations are among the common causes of early onset epileptic encephalopathies, including OS. *KCNQ2* mutations have been shown to cause benign familial neonatal seizures, which is distinct from OS.[2,3] We unexpectedly found *KCNQ2* mutations by whole exome sequencing. Exome sequencing using familial trios (patients and their parents) can identify de novo mutations.[4] Novel associations between unexpected gene mutations and early onset epileptic encephalopathies may be validated by such new technologies.

Acknowledgment

Supported by a research grant from the Ministry of Health, Labor, and Welfare, Japan (H.S., M.K., N.Mi., N.Ma.), a Grant-in-Aid for Scientific Research from the Japan Society for the Promotion of Science (H.S., M.K., N.Mi., N.Ma.), a research grant from the Japan Science and Technology Agency (N.Ma.), and the Strategic Research Program for Brain Sciences (a Grant-in-Aid for Scientific Research on Innovative Areas, Foundation of Synapse and Neurocircuit Pathology; N.Ma.).

Potential Conflicts of Interest

Nothing to report.

[1]*Department of Human Genetics, Yokohama City University Graduate School of Medicine, Yokohama,* [2]*Department of Pediatrics, Yamagata University Faculty of Medicine, Yamagata,* [3]*Department of Neurology, Tokyo Metropolitan Children's Medical Center, Fuchu, and* [4]*Department of Pediatrics, Fukuoka University Faculty of Medicine, Fukuoka, Japan*

References

1. Weckhuysen S, Mandelstam S, Suls A, et al. KCNQ2 encephalopathy: emerging phenotype of a neonatal epileptic encephalopathy. Ann Neurol 2012;71:15–25.
2. Singh NA, Charlier C, Stauffer D, et al. A novel potassium channel gene, KCNQ2, is mutated in an inherited epilepsy of newborns. Nat Genet 1998;18:25–29.

3. Biervert C, Schroeder BC, Kubisch C, et al. A potassium channel mutation in neonatal human epilepsy. Science 1998;279: 403–406.
4. Vissers LE, de Ligt J, Gilissen C, et al. A de novo paradigm for mental retardation. Nat Genet 2010;42:1109–1112.

DOI: 10.1002/ana.23620

Brain Death in Children: Why Does It Have to Be So Complicated?

Thomas Nakagawa, MD,[1] Stephen Ashwal, MD,[2] Mudit Mathur, MD,[3] and Mohan Mysore, MD[4]

The authors appreciate the editorial comments by Wijdicks and Smith[1] and would like to address concerns about why the diagnosis of brain death in pediatric patients has to be "so complicated."

This revised clinical guideline focused specifically on determining brain death and deliberately excluded issues related to ethical concerns and organ donation. Failure to mention the Child Neurology Society (CNS) as the third sponsoring society of this guideline is a major oversight of the editorial.[1] CNS provided significant review by Practice Committee members and the society's Executive Board.[2] The quality of evidence provided in this guideline was equivalent to, if not more comprehensive than, the revised American Academy of Neurology (AAN) guideline, which reported only class III or IV evidence for 4 of 5 questions posed.[3] We used the GRADE system to develop a consensus guideline because no class I or II studies to determine pediatric brain death exist.[2] Interestingly, the AAN is currently revising guideline development for practicing neurologists to use a modification of the GRADE system.

A wide range of clinical entities can result in brain death in newborns, children, and adolescents. The guideline, the checklist, and Table 3 clearly state that all reversible conditions should be excluded prior to the first brain death examination. However, some uncertainty in the newborn period still exists leading to age-based observation periods. These consensus based recommendations reflect extensive clinical experience across several pediatric disciplines. Additionally, provisions for pediatric trauma patients and neonates were included. Virtually every committee member has cared for acutely injured children who met examination criteria for brain death within the initial 24 hours. Some recovered brain function although most did not which is why 2 examinations over defined time periods is recommended. The recommended time periods are consensus based rather than arbitrary time periods. Neurologic examination findings remaining unchanged and consistent with brain death throughout the observation period was one of the recommended criteria for determining brain death in the 1987 guidelines. The committee retained this recommendation in the current update. We agree that apparent neurologic improvements reported in anecdotal cases are due to diagnostic errors when critically examined; this is precisely the reason why a change in findings between examinations implies the neurological process is potentially reversible, precluding the diagnosis of brain death.

The revised guideline repeatedly states that brain death is a clinical diagnosis, and factors influencing the neurologic examination must be corrected before initiating brain death evaluation and apnea testing. Ancillary studies do not trump the neurological examination, and we clearly state that ancillary studies should not be viewed as a substitute for the neurologic examination. However, situations exist where ancillary studies are helpful to determine death. The revised guideline and checklist have simplified and clarified many previous sources of confusion. Additionally, the checklist will help standardize determination and documentation of brain death in children.[4]

Prolonging declaration of death does not appear to be a major concern in children—perhaps differing from the experience in adults. Families appreciate the added certainty conferred by the second examination. Patients in children's hospitals rely on assessments by pediatric specialists who understand the unique needs of children and their families. The approach to caring for children is very different and likely more family centered. These issues are further addressed in the full guideline and we encourage readers to review the entire document published in Critical Care Medicine and Pediatrics.[2,5]

Declaring brain death in children is complicated and should be undertaken by physicians who are adequately trained in the complexities involved in this important determination. We agree more research is needed to address some of the other issues raised in the editorial, and we again thank Drs Wijdicks and Smith for their opinion.

Potential Conflicts of Interest

Nothing to report.

[1]*Departments of Anesthesiology (Section on Pediatric Critical Care) and Pediatrics, Wake Forest School of Medicine, Winston-Salem, NC,* [2]*Department of Pediatrics (Division of Child Neurology) and* [3]*Division of Pediatric Critical Care, Loma Linda University School of Medicine, Loma Linda, CA, and* [4]*Department of Pediatrics, University of Nebraska College of Medicine, Omaha, NE*

References

1. Wijdicks EF, Smith WS. Brain death in children: why does it have to be so complicated? Ann Neurol 2012;71:442–443.
2. Nakagawa TA, Ashwal S, Mathur M, et al. Guidelines for the determination of brain death in infants and children: an update of the 1987 Task Force recommendations. Crit Care Med 2011;39:2139–2155.
3. Wijdicks EF, Varelas PN, Gronseth GS, et al. Evidence-based guideline update: determining brain death in adults: report of the Quality Standards Subcommittee of the American Academy of Neurology. Neurology 2010;74:1911–1918.
4. Fackler J, Goldstein B. Pediatric brain death. Crit Care Med 2011; 39;2197–2198.
5. Clinical report - Guidelines for the Determination of Brain Death in Infants and Children. An Update of the 1987 Task Force Recommendations. Nakagawa TA, Ashwal, SA, Mathur M, Mysore M., and the Committee for Brain Death in Infants and Children. Pediatrics. 2011;128:3 e720-e740. doi: 10.1542/peds.2011-1511.

DOI: 10.1002/ana.23623

Epilepsia, 53(8):1441–1449, 2012
doi: 10.1111/j.1528-1167.2012.03548.x

FULL-LENGTH ORIGINAL RESEARCH

CASK aberrations in male patients with Ohtahara syndrome and cerebellar hypoplasia

***Hirotomo Saitsu, †Mitsuhiro Kato, ‡Hitoshi Osaka, §Nobuko Moriyama, ¶Hideki Horita, *Kiyomi Nishiyama, *Yuriko Yoneda, *Yukiko Kondo, *Yoshinori Tsurusaki, *Hiroshi Doi, *Noriko Miyake, †Kiyoshi Hayasaka, and *Naomichi Matsumoto**

***Department of Human Genetics, Yokohama City University Graduate School of Medicine, Kanazawa-ku, Yokohama, Japan; †Department of Pediatrics, Yamagata University Faculty of Medicine, Yamagata, Japan; ‡Division of Neurology, Clinical Research Institute, Kanagawa Children's Medical Center, Minami-ku, Yokohama, Japan; §Department of Pediatrics, Hitachi, Ltd., Hitachinaka General Hospital, Hitachinaka, Japan; and ¶Department of Pediatrics, Ibaraki Disabled Children's Hospital, Mito, Japan**

Summary

Purpose: Ohtahara syndrome (OS) is one of the most severe and earliest forms of epilepsy. *STXBP1* and *ARX* mutations have been reported in patients with OS. In this study, we aimed to identify new genes involved in OS by copy number analysis and whole exome sequencing.

Methods: Copy number analysis and whole exome sequencing were performed in 34 and 12 patients with OS, respectively. Fluorescence in situ hybridization, quantitative polymerase chain reaction (PCR), and breakpoint-specific and reverse-transcriptase PCR analyses were performed to characterize a deletion. Immunoblotting using lymphoblastoid cells was done to examine expression of CASK protein.

Key Findings: Genomic microarray analysis revealed a 111-kb deletion involving exon 2 of *CASK* at Xp11.4 in a male patient. The deletion was inherited from his mother, who was somatic mosaic for the deletion. Sequencing of the mutant transcript expressed in lymphoblastoid cell lines derived from the patient confirmed the deletion of exon 2 in the mutant transcript with a premature stop codon. Whole exome sequencing identified another male patient who was harboring a c.1A>G mutation in *CASK*, which occurred de novo. Both patients showed severe cerebellar hypoplasia along with other congenital anomalies such as micrognathia, a high arched palate, and finger anomalies. No CASK protein was detected by immunoblotting in lymphoblastoid cells derived from two patients.

Significance: The detected mutations are highly likely to cause the loss of function of the CASK protein in male individuals. *CASK* mutations have been reported in patients with intellectual disability with microcephaly and pontocerebellar hypoplasia or congenital nystagmus, and those with FG syndrome. Our data expand the clinical spectrum of *CASK* mutations to include OS with cerebellar hypoplasia and congenital anomalies at the most severe end.

KEY WORDS: *CASK*, Ohtahara syndrome, Male, Cerebellar hypoplasia.

Ohtahara syndrome (OS), also known as early infantile epileptic encephalopathy with suppression-burst, is one of the most severe and earliest forms of epilepsy (Ohtahara et al., 1976). It is characterized by early onset of seizures, typically frequent epileptic spasms, seizure intractability, characteristic suppression-burst patterns on electroencephalography (EEG), and poor outcome with severe psychomotor retardation (Djukic et al., 2006; Ohtahara & Yamatogi, 2006). Brain malformations such as cerebral dysgenesis, hemimegalencephaly, Aicardi syndrome, and porencephaly are often associated with OS (Yamatogi & Ohtahara, 2002). However, mutations of the *ARX* and *STXBP1* gene have been reported in individuals with OS who showed no brain malformations, indicating that mutated genes are involved in OS (Kato et al., 2007, 2009; Fullston et al., 2010; Giordano et al., 2010; Saitsu et al., 2008, 2010).

CASK (Genbank accession number NM_003688.3) at Xp11.4 encodes a calcium/calmodulin-dependent serine protein kinase of 921 amino acids belonging to the membrane-associated guanylate kinase protein family (Hsueh, 2006). Accumulating evidence indicates that *CASK* is essential for synapse formation at both presynaptic and postsynaptic junctions. In addition, CASK enters the nucleus and regulates expression of genes involved in cortical development (Hsueh, 2006). Recently, heterozygous loss-of-function mutations in *CASK* were found in four female patients with X-linked intellectual disability (ID);

Accepted April 23, 2012; Early View publication June 18, 2012.
Address correspondence to Hirotomo Saitsu, Department of Human Genetics, Yokohama City University Graduate School of Medicine, 3-9 Fukuura, Kanazawa-ku, Yokohama 236-0004, Japan. E-mail: hsaitsu@yokohama-cu.ac.jp

microcephaly and pontocerebellar hypoplasia (MICPCH) and a hemizygous synonymous c.915G>A mutation, which caused skipping of exon 9 of *CASK* in about 20% of the mutant transcripts, was found in a male patient with the same disease and presentation (Najm et al., 2008). To date, 32 additional female cases have been reported, suggesting that ID, MICPCH, growth retardation, axial hypotonia with or without hypertonia of extremities, and optic nerve hypoplasia are caused by loss-of-function mutations of *CASK* in female cases (Moog et al., 2011; Hayashi et al., 2012). On the other hand, a missense mutation causing a partial skipping of exon 2 of *CASK* was found in affected male individuals in an Italian family with FG syndrome, which is characterized by multiple congenital anomalies and ID (Piluso et al., 2009). More recently, five missense mutations and a splice mutation, causing amino acid changes or in-frame deletions of the CASK protein, were found in male patients and variably affected carrier female patients with ID, often accompanied by congenital nystagmus (Tarpey et al., 2009; Hackett et al., 2010). Therefore it has been postulated that hypomorphic *CASK* alleles cause ID in male individuals. Collectively, mutations of *CASK* could cause a wide spectrum of ID, ranging from nonsyndromic mild ID to syndromic severe ID with structural brain abnormalities in both male and female patients.

Herein, we report on two male patients with OS, cerebellar hypoplasia, and multiple congenital anomalies. One patient had a *CASK* deletion and the other had a mutation at the translation initiation codon, both likely leading to a loss of CASK function. Detailed clinical and molecular data are presented.

Methods

Patients

A total of 34 Japanese patients (20 male and 14 female) with OS were analyzed for copy number aberrations. Twelve of them were additionally analyzed by whole exome sequencing. The diagnosis was made based on clinical features and characteristic patterns on EEG. Mutations in *STXBP1* were not identified in these patients (including Patients 1 and 2) by high-resolution melting analysis. Thirteen male patients, including Patient 1, and three female Patients were negative for *ARX* mutation. The experimental protocols were approved by the Yokohama City University School of Medicine Institutional Review Boards for Ethical Issues. Written informed consent was obtained from all individuals and/or their families in compliance with the relevant Japanese regulations.

Genomic microarray and cloning of deletion breakpoint

Genomic DNA obtained from peripheral blood leukocytes was used. Copy number alterations were studied by using Cytogenetics Whole-Genome 2.7M Array (Affymetrix, Santa Clara, CA, U.S.A.) for 30 patients and GeneChip Human Mapping 250K NspI (Affymetrix) for four patients. Copy number alterations were analyzed using the Chromosome Analysis Suite (ChAS; Affymetrix) with NA30.1 (hg18) annotations (for 2.7M Array) or using CNAG2.0 (for 250K) (Nannya et al., 2005). The junction fragment spanning the deletion was amplified by long polymerase chain reaction (PCR), using several primer sets based on putative breakpoints from the microarray data. The junction fragment was amplified using following primers: forward, 5′-ACCCAGCGTTTCACCAAGGTCTCT-3′; reverse, 5′-GTGGCTTCAGAATTAGGCCCACAAA-3′ (product size = 1,136 bp). PCR products were electrophoresed in agarose gels, stained with ethidium bromide, extracted from the gels using a QIAquick Gel extraction kit (Qiagen, Tokyo, Japan), and sequenced.

Quantitative real-time PCR

The deletion of *CASK* was analyzed using the patient's and parental genomic DNA by quantitative real-time PCR (qPCR) on a Rotor-Gene Q thermal cycling system (Qiagen). DNA extracted from two independent blood samples each from the patient and mother were used for analysis. PCR was performed in a volume of 15 μl containing 10 ng of genomic DNA, 1× Rotor-Gene SYBR Green PCR Master Mix (Qiagen), and 1.0 μM each primer. qPCR was carried out using the two standard curve relative quantification method with four standard samples including 30, 10, 3.33, and 1.11 ng DNA, respectively. Three primer sets for exons 2, 3, and 4 of *CASK*, and one reference primer set for an area on chromosome 9 were used. Relative copy number of test regions was calculated in comparison with that of the reference region. The experiments were independently repeated three times. The data were averaged, and the standard deviation was calculated. Primer information is available on request.

Fluorescent in situ hybridization (FISH)

RP11-977L20 covering the deletion of *CASK* was labeled with SpectrumGreen -11-dUTP (Abbott, Tokyo, Japan) by nick translation. Probe-hybridization mixtures (15 μl) were denatured at 70°C for 5 min, applied to chromosomes, incubated at 37°C for 20 h, and then washed and mounted with antifade solution (Vector Laboratories, Burlingame, CA, U.S.A.) containing 4,6-diamidino-2-phenylindole. Photographs were taken on an AxioCam MR Charge Coupled Device camera fitted to an Axioplan2 fluorescence microscope (Carl Zeiss, Tokyo, Japan). The mosaic ratio was examined by two independent investigators, who each counted 100 interphase nuclei.

RNA analysis

RNA analysis using lymphoblastoid cell lines was performed as described previously (Saitsu et al., 2011). Briefly, total RNA was extracted using an RNeasy Plus Mini Kit (Qiagen); 2 μg of total RNA was subjected to reverse transcription, and 1 μl of cDNA was used for PCR.

Primer sequences are ex1-F (5′-ATGTGTACGAGCTGT GCGAGGTGAT-3′) and ex4-R (5′-AGCGTCAGCTCGCT TTACGATTTCA-3′). Two separately extracted RNA samples were used in each duplicated experiment. The DNA in each PCR band was purified using a QIAquick Gel extraction kit (Qiagen) and sequenced.

Whole exome sequencing

DNAs were captured using the SureSelect^{XT} Human All Exon 50 Mb Kit (Agilent Technologies, Santa Clara, CA, U.S.A.) and sequenced with one lane per sample on an Illumina GAIIx platform (Illumina, San Diego, CA, U.S.A.) with 108-bp paired-end reads. Image analysis and base calling were performed by sequence control software real-time analysis and CASAVA software v1.7 (Illumina). A total of 94,106,348 paired-end reads were obtained for Patient 2 and aligned to the human reference genome sequence (GRCh37/hg19) using MAQ (Li et al., 2008) and NextGENe software v2.00 with sequence condensation by consolidation (SoftGenetics, State College, PA, U.S.A.). Single nucleotide variants (SNVs) were called using MAQ and NextGENe. Small insertions and deletions were detected using NextGENe. Called SNVs were annotated with SeattleSeq Annotation. The number of variants identified by exome sequencing in Patient 2 is shown in Table S1.

Immunoblotting

Lymphoblastoid cells were washed twice in ice-cold phosphate-buffered saline (PBS), and lysed in sodium dodecyl sulfate sample buffer. Samples were size-fractionated by sodium dodecyl sulfate–polyacrylamide gel electrophoresis, transferred to the polyvinylidene fluoride membrane, and analyzed with anti-CASK monoclonal antibody, which is produced by a synthetic peptide corresponding to residues surrounding Glu327 of human CASK protein (1:1,000 dilution, D24B12; Cell Signaling, Tokyo, Japan). Anti-Lamin B polyclonal antibody (1:500 dilution, sc-6217; Santa Cruz Biotechnology Inc., Santa Cruz, CA, U.S.A.) was used as a control. Secondary antibody was peroxidase-conjugated goat anti-rabbit IgG or bovine anti-goat IgG (Jackson ImmunoResearch, West Grove, PA, U.S.A.). Blots were detected using the Supersignal West dura (Pierce, Yokohama, Japan). Chemiluminescence was visualized using a FluorChem 8900 (Alpha Innotech, San Leandro, CA, U.S.A.). Experiments were repeated twice using two separately prepared samples.

Results

Clinical information

Patient 1 is a 4-year-old boy born to nonconsanguineous parents. The pregnancy was uneventful, and he was born at term (gestational age 41 weeks and 2 days) with induced labor but no asphyxia. His body weight was 2,606 g (−2.0 standard deviation [SD]), his height was 47.5 cm (−1.4 SD), and his head circumference was 32.2 cm (−1.2 SD). An apneic event with cyanosis, which was not improved by positioning or oxygen inhalation, was evident 2 days after birth. Brain magnetic resonance imaging (MRI) demonstrated prominent cerebellar hypoplasia (Fig. 1A). EEG showed multifocal epileptic discharges with a short period (1 s) of flat basic rhythm (Fig. 1C, left). Phenobarbital was administered at 21 days and was effective for the apneic event. At the age of 2 months, he developed daily clustering of tonic seizures with suppression-burst pattern on both awake and asleep EEG (Fig. 1C, right)and poor feeding. EEG at 5 months demonstrated hypsarrhythmia, which is characteristically seen in West syndrome. He exhibited long slender fingers, micropenis, micrognathia, and a short neck with obstructive respiration, and then required tracheostomy with laryngotracheal separation and gastrostomy. His head circumference was 47.1 cm (−2.7 SD) at 1 years and 4 months. On examination at 4 years, he was bedridden and unable to track objects. Tonic seizures lasting 10–30 s several times a day and frequent myoclonic seizures were seen regardless of treatment with phenobarbital, pyridoxal phosphate, zonisamide, clobazam, and lamotrigine. EEG during sleep at 3 years of age demonstrated multifocal sharp and slow-wave complexes and diffuse low-voltage fast-wave bursts or a desynchronization pattern.

Patient 2 is a 4-year-old boy born to nonconsanguineous parents. He was born at 39 weeks of gestation without asphyxia after uneventful pregnancy. His body weight was 2,000 g (−3.3 SD), his height was 43.0 cm (−2.8 SD), and his head circumference was 29.5 cm (−2.7 SD). He was poorly fed with milk and referred to us at 27 days after birth. Multiple anomalies were recognized such as micrognathia, high arched palate, shortened upper arms, bilateral overlapping fingers and clinodactyly, and persistent hypertrophic primary vitreous. He underwent ophthalmic surgery at 33 days after birth. Brain MRI demonstrated prominent cerebellar hypoplasia (Fig. 1B). At 3 months of age, he showed frequent generalized tonic seizures, and EEG showed a suppression-burst pattern in both awake and asleep states (Fig. 1D). He showed normal auditory brain responses. Laboratory data, including lactate, pyruvate, and very long fatty acids, were all normal. Phenobarbital was initiated and only partially effective for his seizures. Topiramate, clobazam, and sodium bromide were added, and seizure frequencies were decreased from daily to weekly. His development was severely delayed with no head control or eye pursuit. His deep tendon reflexes are exaggerated, with positive bilateral Babinski signs. He shows muscle hypertonus with rigidity of both upper and lower limbs.

Copy number analysis

Through screening for copy number alterations by genomic microarray analysis, we identified an approximately 110-kb microdeletion involving exon 2 of *CASK* at Xp11.4 in Patient 1 (Fig. 2A). Breakpoint-specific PCR analysis of

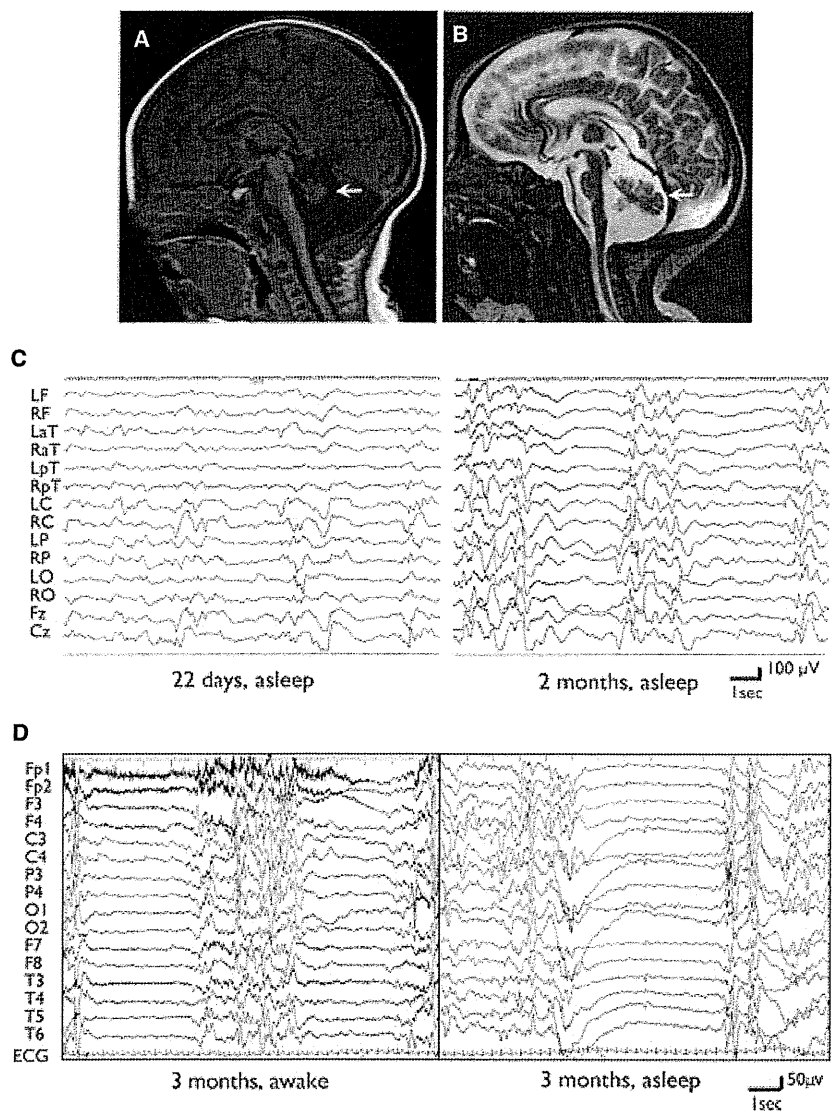

Figure 1.
Brain MRI findings in the patients. (**A**) T_1-weighted midline sagittal image of Patient 1 at age 21 days. (**B**) T_2-weighted midline sagittal image of Patient 2 at age 3 months. Both patients showed prominent cerebellar hypoplasia (arrows). (**C**) EEG of Patient 1 showed multifocal sharp wave or irregular sharp-and-slow wave complex but no diffuse epileptic discharges at age 22 days (left) and diffuse high-amplitude slow-wave burst mixed with irregular spike or sharp wave interrupted by low-amplitude activity (suppression-burst) at age 2 months (right). (**D**) EEG of Patient 2 at age 3 months. High-voltage bursts alternate with almost flat suppression phases at an approximately regular rate in both awake and asleep states.
Epilepsia © ILAE

the family showed that the deletion was inherited from his mother (Fig. 2B). The sequence of the junctional fragment confirmed a 111,172-bp deletion (NG_016754.1: g.17883_129055del) (Fig. 2C). Sequencing also identified 5-bp duplicated sequences as well as a 2-bp insertion at the deletion junction. We were surprised that the healthy mother possessed this deletion, because the deletion is predicted to lead to a frameshift with presumably premature termination of the translation. The deletion was further examined by qPCR and FISH analyses. Whereas the relative copy numbers of exons 3 and 4 (not deleted) were nearly 1.0 in the two maternal DNA samples, as expected, those for deleted exon 2 in the two samples were 0.67 and 0.81 (Fig. 2D). Because the relative copy number is expected to be 0.5 if one of two copies is deleted (as the healthy father showed), this result suggested that the mother may be somatic mosaic for the deletion. In fact, FISH analysis revealed that only 40 of 200 interphase nuclei showed one clear signal and another weaker signal, consistent with partial deletion within the bacterial artificial chromosome probe (Fig. 2E). Based on these findings, we concluded that the mother is somatic mosaic for the deletion, and that the percentage of mosaicism is approximately 20%. To explore the effect of the deletion on the transcription of *CASK*, reverse transcriptase PCR designed to amplify exons 1–4 was performed using total RNA extracted from lymphoblastoid cell lines (LCLs) derived from the patient and his mother (Fig. 2F). A single band (299-bp) corresponding to the wild-type *CASK* allele was amplified using a complementary DNA (cDNA) template from a control LCL (Fig. 2F). By contrast, only a smaller band, in which exon 2 had been deleted, was detected from the patient's cDNA

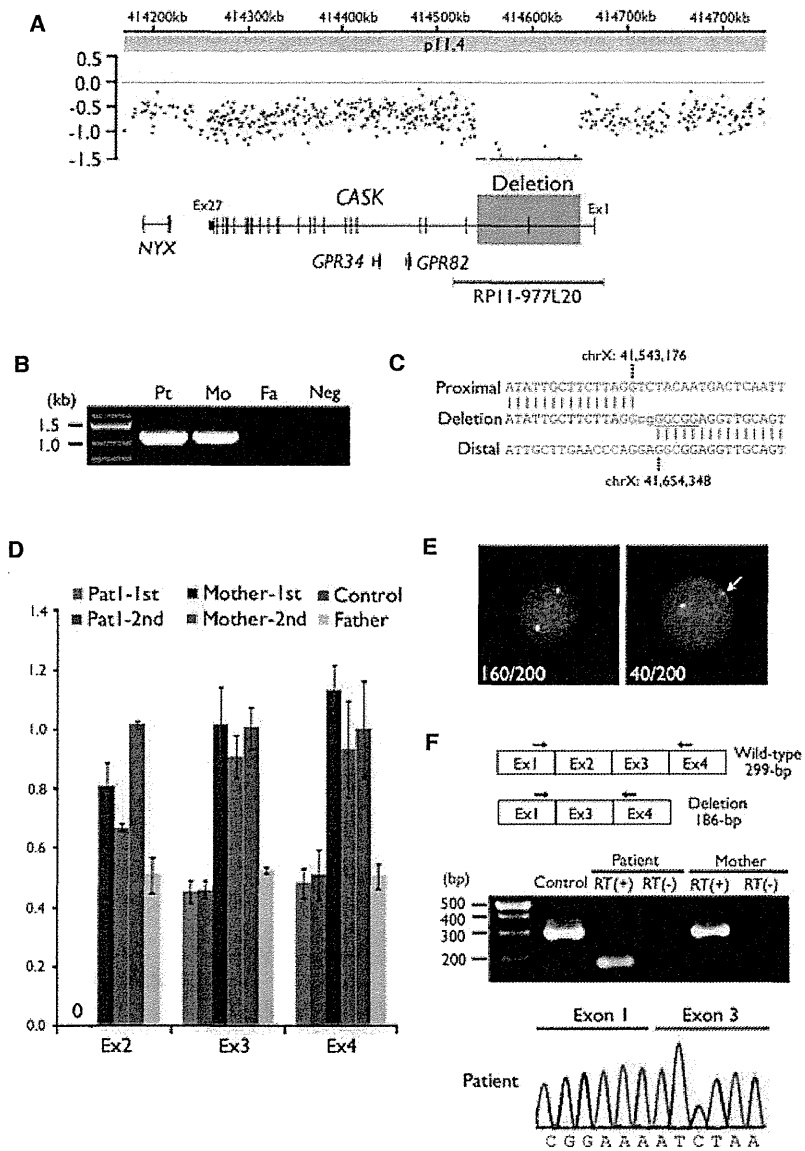

Figure 2.

A 111-kb deletion involving exon 2 of *CASK*. (**A**) The 2.7M array profile clearly shows a deletion involving exon 2 of *CASK* at Xp11.4. The x- and y-axes show the genomic location from the p telomere of chromosome X (UCSC coordinates, May, 2006) and $\log_2$ signal ratio values, respectively. Four RefSeq genes including *CASK* and RP11-977L20 clone used for FISH are shown. (**B**) Breakpoint-specific PCR analysis of the family. Primers flanking the deletion were able to amplify a 1,136-bp product from both the Patient 1 and his mother. Pt, patient; Mo, mother; Fa, Father; Neg, negative control (no template DNA). (**C**) Deletion junction sequence. Top, middle, and bottom strands show proximal, deleted and distal sequences, respectively. The two nucleotides inserted are presented in lower case. A 5-bp sequence that appears twice at the breakpoint region is colored red or underlined. (**D**) qPCR analysis of the family, and a female control. Two DNA samples extracted from two independent blood samples were used for analysis of the patient and his mother. Relative copy numbers of deleted exon 2 were 0.67 and 0.81 (both above 0.5) in the mother, suggesting somatic mosaicism of the deletion. (**E**) FISH images of RP11-977L20, covering the deletion, on the mother's chromosomes. One-hundred sixty nuclei showed two clear signals (left), and 40 nuclei showed one clear signal and a weaker signal (right, white arrow) consistent with partial deletion within the probe. (**F**) Schematic representation of the transcript from exons 1–4 of *CASK*. Exons and primers are depicted as boxes and arrows, respectively (top). A single wild-type amplicon was detected in a control and the mother. A smaller product was amplified only from the patient's cDNA. RT (+): with reverse transcriptase, RT (–): without reverse transcriptase as a negative control. Sequence of a smaller amplicon clearly demonstrated the exon 2 deletion (bottom).